Understanding Mott's law from scaling of variable-range-hopping currents and intrinsic current fluctuations

W. F. Pasveer* and M. A. J. Michels†
Group Polymer Physics, Eindhoven Polymer Laboratories and Dutch Polymer Institute, Technische Universiteit Eindhoven, P.O. Box 513, 5600 MB Eindhoven, The Netherlands

(Received 22 May 2006; revised manuscript received 5 October 2006; published 30 November 2006)

We have used the master equation to simulate variable-range hopping (VRH) of charges in a strongly disordered d-dimensional energy landscape ($d=1,2,3$). The current distribution over hopping distances and hopping energies gives a clear insight into the difference between hops that occur most frequently, dominate quantitatively in the integral over the mobility distribution, or are critical ones that still need to be considered in that integral to recover the full low-temperature mobility. The recently reported scaling with temperature of the VRH-current distribution over hopping distances and hopping energies is quantitatively analyzed in 1D and 2D, and accurately confirmed. Based on this, we present an analytical scaling theory of VRH, which distinguishes between a scaling part of the distribution and an exponential tail, separated by critical currents that set the scale and that follow self-consistently at each temperature. This naturally renders Mott's law for the low-temperature mobility, in a way and with a physical picture different from that of the established critical-percolation-network approach to VRH. We argue that current fluctuations as observed in simulations are intrinsic to VRH and play an essential role in this distinction.

DOI: 10.1103/PhysRevB.74.195129 PACS number(s): 72.20.Ee, 72.10.−d, 72.80.Ng

I. INTRODUCTION

The low-temperature charge mobility in disordered conductors continues to receive much attention both experimentally and theoretically.[1–11] As shown already by Mott,[12] this mobility can be understood to result from thermally assisted variable-range hopping (VRH) between localized states of varying energy. Mott thereby considers a single-hop rate of the form $\exp(-\alpha R-\beta\varepsilon)$ (α is the inverse localization length and $\beta=1/k_BT$) first introduced by Miller and Abrahams,[13] which accounts both for tunneling through the tail of the wave function and for a phonon-assisted thermal activation. At low temperatures, a compromise has to be sought between hopping distances R well beyond the nearest-neighbor distance and hopping energies ε well above k_BT, to reach a percolating conduction path through the bulk disordered medium. By identifying the bulk mobility μ^* with the probability of a single critical hop for persistent transport Mott derived a dominant temperature dependence (apart from logarithmic corrections) of the form

$$\log \mu^* = -(T_0/T)^{\gamma}, \tag{1}$$

with

$$k_BT_0 = a(d)\alpha^d/\varrho_F, \tag{2}$$

and with $\gamma\equiv 1/(d+1)$; $a(d)$ is a constant of order unity, ϱ_F the (constant) density of states at the Fermi level, and d the spatial dimension.

The universal softer-than-activated temperature-dependent mobility given by Mott's law has been accurately verified experimentally for widely different classes of materials and broad ranges of temperatures (although it should be added that at very low temperatures often an exponent $\gamma=1/2$ is found even in the case of three-dimensional hopping; the latter observation indicates so-called Efros-Shklovskii hopping,[14] in which Coulomb interactions become dominant in the hop and induce a gap in the density of states). However, the theoretical understanding of Mott's law has been a subject of much discussion. To improve upon Mott's choice of representing the statistical and highly disordered transport process by a single critical hop, several authors[15–17] have mapped the problem onto a mean-field random-resistor network and used a percolation approach to calculate the network mobility. In this approach, bonds are artificially introduced in the $(d+1)$-dimensional VRH space of site position and energy in decreasing order of conductance, until at a minimum conductance a first continuous path is reached, which should correspond with the Mott percolation point. The minimum bond conductance is then identified with the bulk conductance, while bonds of still lower conductance are supposed to become short-circuited, and are left out.

Very recently, extensive simulations of VRH currents have been reported which give a detailed insight into the distribution of VRH currents in the two-dimensional space of hopping distances and hopping energies.[18] In particular, this work numerically reveals a scaling of the VRH currents, in such a form that the normalized distribution of currents over the two-dimensional space of random-resistor variables depends on temperature only via a dimensionless parameter $l\equiv(\alpha^d\beta/\varrho_F)^{\gamma}$; this parameter is proportional to Mott's critical parameters $\alpha R_M(\beta)$ and $\beta\varepsilon_M(\beta)$, and is used in Ref. 18 to scale the random-resistor distances and energies. In view of Mott's analysis, such temperature dependence may be expected for the parameters of some typical hop derived from the distribution, but the striking result of Ref. 18 is that the scaling actually turns out to hold for a large area in parameter space around the mean. Only for very low values of the conductances the numerical scaling is seen to break down; typically this happens beyond the critical value below which in the percolation approach currents are assumed to be negligible. This suggests a deeper relation between Mott's law,

the percolation approach, and the scaling of the VRH currents, but no such relation has been established in Ref. 18. Rather, the results in Ref. 18 for the 3D system seemed to indicate that a non-negligible part of the current distribution still persisted beyond the critical percolation boundary, even for $T \to 0$. A second major result from the recent paper is that the simulated VRH chemical potentials and currents show a marked pattern of spatial fluctuations, which qualitatively appears to scale again in accordance with Mott's parameters.

In Ref. 18, a general scale-transformation argument has been given to understand the scaling with the dimensionless parameter l, but this still leaves three fundamental questions unanswered. First, to understand the relation between this scaling and Mott's law; second, to clarify the relation with the percolation approach, including the apparent convergence problems mentioned above; and third, to understand the origin and effect of the current fluctuations in the picture of variable-range hopping. The objective of the present paper is to come to answers to all three fundamental questions. To do so, we will first present more extensive simulation data, gathered by the same methods as in Ref. 18, but analyzed in variables that do not assume a random-resistor network and also allow faster convergence for low temperatures. Second, we rationalize the scaling data in terms of an analytical scaling theory of VRH, with a physical picture distinct from the established critical-percolation-network argument. Third, we will argue that fluctuations intrinsic to VRH play a natural role in this distinction.

II. SIMULATION METHOD

To simulate the VRH currents we follow the same master-equation approach as in Ref. 18 (see also Refs. 19–21). We first generate randomly distributed energies on each site of an array of lattice constant R_0 and size L^d, $d=1,2,3$, by sampling from an interval $|\varepsilon| \leqslant \varepsilon_0/2 \equiv (2R_0^d \varrho_F)^{-1}$. (Note that disorder is here only energetic; we can choose a regular lattice since in the limit that we are interested in the hop lengths will be much larger than the lattice constant. Positional disorder is important however beyond the Ohmic regime.[22]) Charges are introduced by setting the chemical potential in the Fermi-Dirac (FD) distribution zero. Then we apply an electric field in the x-direction and solve the steady-state Kirchhoff equation for the FD occupation numbers n_i, with sites i having position vectors $\mathbf{R}_i$ and energies ε_i. The effective mobility then follows as

$$\langle n_i^0 \rangle \mu^* \mathbf{E} = L^{-d} \sum_{i<j} \mathbf{R}_{ij} [W_{ij} n_i (1-n_j) - (i \leftrightarrow j)]. \tag{3}$$

Here the angular brackets represent a sample average, n_i^0 is the equilibrium occupation number, and W_{ij} the Miller-Abrahams transition rate[13]

$$W_{ij} = \begin{cases} \nu_0 \exp[-\alpha|\mathbf{R}_{ij}| - \beta(\varepsilon_j - \varepsilon_i)], & \varepsilon_j > \varepsilon_i, \\ \nu_0 \exp(-\alpha|\mathbf{R}_{ij}|), & \varepsilon_j < \varepsilon_i, \end{cases} \tag{4}$$

with ν_0 an intrinsic rate; ε includes a contribution $-q\mathbf{E}\cdot\mathbf{R}$ from the external field $\mathbf{E}$, q being the particle charge. Within the mentioned random-resistor description, the left hand of Eq. (3) is written in terms of the sample conductance G^*, while the hopping-rate factor between square brackets at the right-hand side can be replaced by a product of a local conductance G_{ij} and a potential difference V_{ij}; Eq. (3) then takes the form

$$(L^{2-d} R_0^2/q) G^* \mathbf{E} = L^{-d} \sum_{i<j} \mathbf{R}_{ij} G_{ij} V_{ij} = \langle \mathbf{R}_{ij} G_{ij} V_{ij} \rangle. \tag{5}$$

Using this equality, the random-resistor-percolation approach identifies the bulk conductance G^* with some critical minimum conductance level $G_{ij,c}$ that is needed to achieve percolation upon sequential introduction of all G_{ij} in decreasing order; obviously this leaves ambiguity in the associated hop length $|\mathbf{R}_{ij}|$ in the average (5).

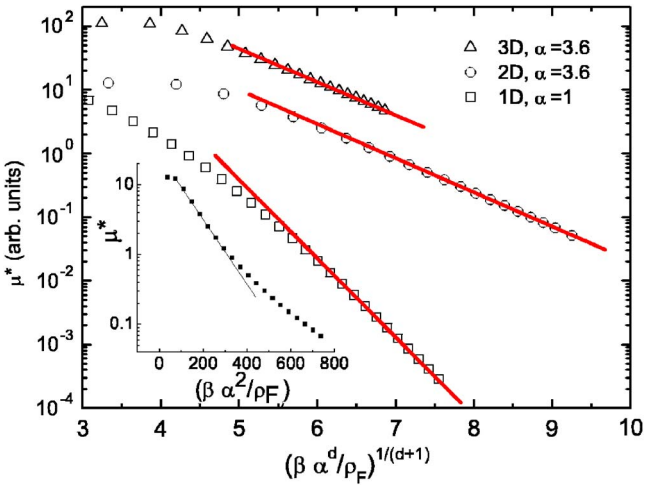

FIG. 1. (Color online) Mobility as a function of temperature for three spatial dimensions. Array sizes L^d used for calculations: $L=10\,000$, 200, and 60 for $d=1,2,3$, respectively. The number of neighbors N taken into account is $N=79,99,215$ for $d=1,2,3$. Averaging over different disorder realizations is performed to get error bars smaller than the symbol size; for $d=3$ the error bar is of the order of the symbol size. The inset shows the 2D high-T activated behavior.

III. NUMERICAL RESULTS

To show the numerical results of our master-equation simulation for the temperature dependence of the mobility we introduce units $q=R_0=\nu_0=\varepsilon_0=1$.

Figure 1 confirms that in each dimension μ^* follows a straight line for low temperatures only if the temperature is plotted as $\beta^{1/(d+1)}$, a direct consequence of Mott's VRH. This has already been shown by McInnes and Butcher.[21] The slopes of the curves give prefactors $a(d)=2.81, 1.24, 1.20$ for the relation between $k_B T_0$ and α^d/ϱ_F.

Our simulations enable us to see what actually happens in (R,ε) space by writing

$$\mu^*(\beta) = \int d\mathbf{R} d\varepsilon \mu(R,\varepsilon;\beta), \tag{6}$$

with the distribution $\mu(R,\varepsilon;\beta)$ following from the summand in Eq. (3). Figure 2 shows typical examples of the distribu-

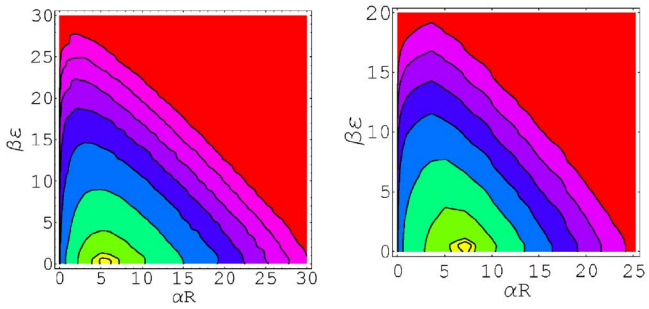

FIG. 2. (Color online) Distribution of hops $(\alpha R, \beta\varepsilon)$ and their contribution to the mobility at a fixed temperature. The left-hand picture shows the situation for $d=1$, $\alpha=1$, $(\beta\alpha/\varrho_F)^{1/2}=7.3$, and the right-hand side for $d=2$, $\alpha=3.6$, $(\beta\alpha^2/\varrho_F)^{1/3}=9.3$. Both plots are normalized on the peak and have contour lines with decreasing values: 0.9, 0.5, 0.1, and then one per decade.

tion in 1D $[\alpha=1,\ (\beta\alpha/\varrho_F)^{1/2}=7.3]$ and 2D $[\alpha=3.6,\ (\beta\alpha^2/\varrho_F)^{1/3}=9.3]$. The continuous contour lines have been generated from the simulation data by a Mathematica interpolation routine. Clearly, our results for 1D and 2D are similar, but we will mainly focus on 2D because the 1D case is known to show possible finite-size peculiarities as pointed out first by Lee[23] and Serota, Kalia, and Lee.[24] Because of computational demand, the 3D distribution has not been thoroughly investigated, but it looks qualitatively the same.

Our detailed results distinguish between hops that are dominant, critical, or most frequent. Figure 2 clearly shows peaks at $(R_p,0)$ giving the *dominant* contribution to the mobility; the figures have mirror images for $\varepsilon<0$, understandable from energy conservation. Around the peak the distribution falls off slower than exponentially, and only for large $\alpha R+\beta\varepsilon$ equidistant lines reflecting the Miller-Abrahams exponential decay can be recognized. We note that, if the slopes in Fig. 1 are to be attributed to *critical* hops (R_M,ε_M), then for $d=2$, $\alpha=3.6$, $(\beta\alpha^2/\varrho_F)^{1/3}=9.3$, we have $\alpha R_M+\beta\varepsilon_M=11.5$, far from the maximum at $(\alpha R_p,\beta\varepsilon_p)=(7.0,0)$ in Fig. 2 and in the region where the logarithmic contours become equidistant.

From mobility distributions at higher temperatures it is seen that the peak then shifts to smaller distances. To study the full (R,ε) picture as a function of temperature, we have scaled in Fig. 3 the distributions $\mu(R,\varepsilon;\beta)$ of two higher temperatures $[d=2,\ \alpha=3.6,\ (\beta\alpha^2/\varrho_F)^{1/3}=7.2$ and $8.8]$ to the data of Fig. 2 by plotting $\mu_{\text{scaled}}\equiv\mu/\mu^*$ vs scaled variables $R_{\text{scaled}}\sim\alpha R\beta^{-1/(d+1)}$, $\varepsilon_{\text{scaled}}\sim\varepsilon\beta^{d/(d+1)}$. Strikingly, the contours from different temperatures coincide both in the peak position and in a much larger (R,ε) domain around it. In fact, significant deviations from this scaling behavior only emerge when $\alpha R+\beta\varepsilon$ approaches values where the logarithmic contours become equidistant, values which in Fig. 2 were identified as critical. Obviously, beyond these critical values the exponential decay precludes scaling. The cross over from the scaling regime to the exponential regime, around the critical Mott values, is first observed at the highest temperature. The above results in particular confirm in quantitative detail the observations of scaling reported in Ref. 18, though in a different energy variable.

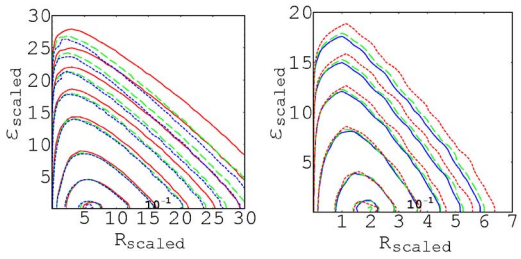

FIG. 3. (Color online) Scaled hop rate $\mu_{\text{scaled}}(R_{\text{scaled}},\varepsilon_{\text{scaled}})$ (contour lines are normalized to the peak, and from 10^{-1} decreasing per decade) for three different temperatures in the Mott regime. Left-handed contour plot shows $(d=1,\ \alpha=1)$: $(\beta\alpha/\varrho_F)^{1/2}=5.3$ (solid line), 6.6 (dashed line), and 7.3 (dotted line) and right-handed contour plot shows $(d=2,\ \alpha=3.6)$: $(\beta\alpha^2/\varrho_F)^{1/3}=7.2$ (dotted line), 8.8 (dashed line), and 9.3 (solid line).

To better visualize the effective jump *frequency* of the diffusive hops one may alternatively plot μ/R^2 rather than μ. We have done so in Fig. 4 for the temperature-scaled data, where for better accuracy we have chosen 1D results only. In this plot for the jump frequency the peak disappears and the distribution increases to a constant near the origin, showing that this is the region of the *most-frequent* hops. Beyond the critical hops, where the contour lines are equidistant, the straightness of these frequency contours is particularly noteworthy; it suggests that in this regime of unlikely hops the jump rate μ/R^2 accurately depends on the sum of the dimensionless hopping variables $\alpha R,\beta\varepsilon$ only.

IV. DERIVATION OF MOTT'S LAW

Let us now rationalize these findings, and in particular show how they imply Mott's law. A natural energy scale in the problem is $\varepsilon_0=(R_0^d\varrho_F)^{-1}$, where ϱ_F is the (constant) density of states near the Fermi level ε_F. For $\beta\varepsilon_0\lesssim 1$ there is nearest-neighbor hopping, but for $\beta\varepsilon_0\gg 1$ the charge carrier

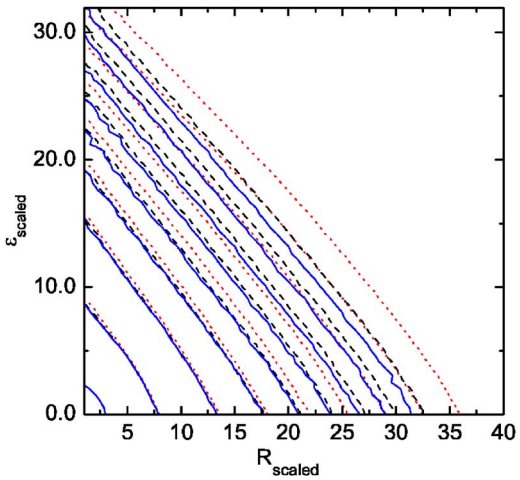

FIG. 4. (Color online) Scaled hop rate $\mu_{\text{scaled}}/R^2_{\text{scaled}}$ (contour lines per decreasing decade with respect to origin) for three different temperatures in the Mott regime $(d=1,\ \alpha=1)$: $(\beta\alpha/\varrho_F)^{1/2}=5.3$ (dotted line), 6.6 (dashed line), and 7.3 (solid line).

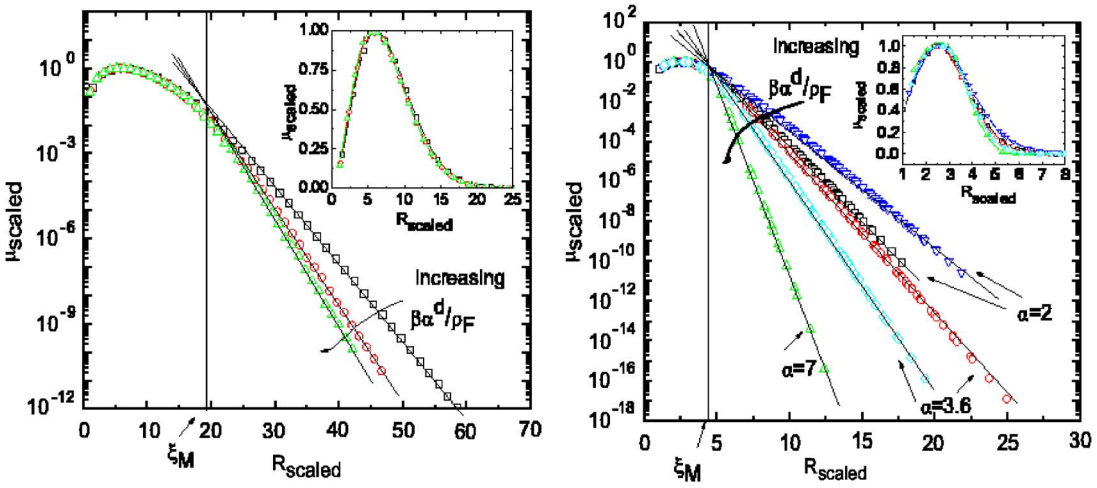

FIG. 5. (Color online) Cross section along $|\varepsilon|=0$ of the scaled distribution $\mu_{\text{scaled}}(R_{\text{scaled}},\varepsilon_{\text{scaled}})$ for ($d=1$, left): $\alpha=1$ and $(\beta\alpha/\varrho_F)^{1/2}=5.3$ (squares), 6.6 (circles), 7.3 (triangles); for ($d=2$, right): $\alpha=2$ and $(\beta\alpha^2/\varrho_F)^{1/3}=5.3$ (down triangles), 6.5 (squares), $\alpha=3.6$ and $(\beta\alpha^2/\varrho_F)^{1/3}=7.2$ (circles), 9.3 (diamonds), $\alpha=7$ and $(\beta\alpha^2/\varrho_F)^{1/3}=17$ (up triangles). The inset shows the same plots but represented in a linear fashion.

is forced to hop further away to find a percolating path. If, like Mott stated, there are maximum hops, characterized by $R_M(\beta)$ and $\varepsilon_M(\beta)$, that still contribute, we can make the following two assumptions: (a) for (R,ε) beyond this maximum we have a contribution $\mu\equiv\mu_>$ that becomes negligible, and (b) in the remaining (R,ε) space the only relevant scales in the contributions to $\mu\equiv\mu_<$ are R_M and ε_M. Supported by Figs. 2 and 3 we can make these assumptions explicit in the following scaling ansatz:

$$\mu_<(R,\varepsilon;\beta)/\mu^*(\beta)=\varrho_F h\left[\frac{R}{R_M(\beta)},\frac{|\varepsilon|}{\varepsilon_M(\beta)}\right],$$

$$\mu_>(R,\varepsilon;\beta)/\mu_0=\varrho_F(\alpha R)^2\exp(-\alpha R-\beta|\varepsilon|). \tag{7}$$

Here $h(x,y)$ is a scaling function which is of order unity in the central part of (R,ε) space. The denominator μ^* in the expression for $\mu_<$ is the self-consistent and T-dependent mobility scale in the (R,ε) domain of relevant hops, while the denominator μ_0 in the expression for $\mu_>$ sets the natural scale of the mobility via an intrinsic T-dependent factor. It may be easily verified that expressions exactly of these forms are implicit in a self-consistent effective-medium theory of VRH;[25] in that case $h(x,y)$ is a trivial function.

Given the expressions for the different regimes, the requirement of continuity at the crossover dictates

$$\mu_<(R_M,\varepsilon_M;\beta)=\mu_>(R_M,\varepsilon_M;\beta), \tag{8}$$

or, with Eq. (7),

$$\mu^*(\beta)=\mu_0\frac{(\alpha R_M)^2}{h(1,1)}\exp(-\alpha R_M-\beta\varepsilon_M). \tag{9}$$

So, the temperature dependence of the mobility $\mu^*(\beta)$ is indeed via an exponential dependence on the scaling parameters $\alpha R_M(\beta)$ and $\beta\varepsilon_M(\beta)$, as supposed by Mott; however, with an additional factor $(\alpha R_M)^2/h(1,1)$, which is temperature-dependent and numerically may be considerably larger than unity.

In view of the symmetry between $\alpha R_M(\beta)$ and $\beta\varepsilon_M(\beta)$ in determining the upper boundary of the scaling regime we argue that there is in fact one scaling parameter: $\alpha R_M(\beta)=\beta\varepsilon_M(\beta)\equiv\xi_M(\beta)$, so the mobility (9) becomes

$$\mu^*(\beta)=\mu_0\frac{[\xi_M(\beta)]^2}{h(1,1)}\exp[-2\xi_M(\beta)]. \tag{10}$$

The β-dependence of $\xi_M(\beta)$ then follows from the self-consistency requirement that in the low-temperature limit $\mu^*(\beta)$ should be recovered by restricting Eq. (6) to the integral over $\mu_<(R,\varepsilon;\beta)$ only, i.e., to the scaling area

$$(1-\eta)\mu^*(\beta)=\int_{\alpha R+\beta|\varepsilon|<2\xi_M} d\mathbf{R}d\varepsilon\,\mu_<(R,\varepsilon;\beta), \tag{11}$$

with the residue η vanishing in that limit. This condition should correspond to the Mott percolation condition, since around percolation a first new natural scale enters the problem. The result is

$$\xi_M(\beta)=\left[\frac{(1-\eta)}{H}\frac{\alpha^d\beta}{\varrho_F}\right]^\gamma\approx l(\beta)/H^\gamma\sim\beta^\gamma,\quad \eta\to 0, \tag{12}$$

with $\gamma=1/(d+1)$, $l(\beta)=(\alpha^d\beta/\varrho_F)^\gamma$, and

$$H(d)\equiv\int_{|\mathbf{x}|+|y|<2} d\mathbf{x}\,dy\,h(x,y). \tag{13}$$

The combination of Eqs. (10) and (12) renders Mott's law (1), with an additional algebraic temperature dependence via the prefactor. Comparison of Eqs. (2), (10), and (12) yields for the numerical constant in Eq. (2): $a(d)=2^{1/\gamma}/H(d)$.

To validate the scaling ansatz (7) quantitatively, we show in Fig. 5 cross sections through scaled current distributions $\mu_{\text{scaled}}(R_{\text{scaled}},\varepsilon_{\text{scaled}})$ along $\varepsilon=0$, for a variety of parameter

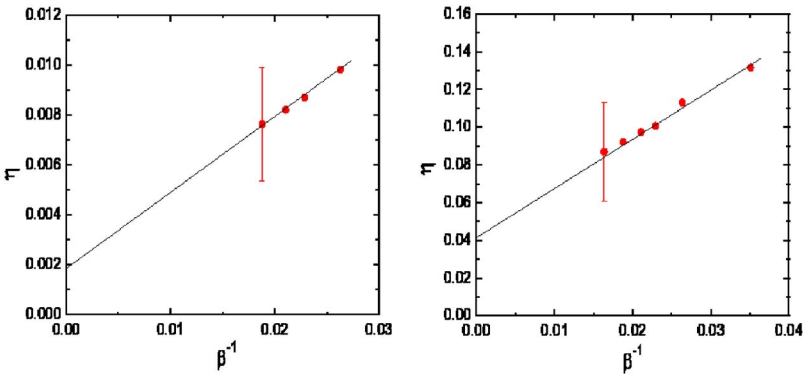

FIG. 6. (Color online) The left-hand graph shows the temperature dependence of η for the 1D case with $\alpha=1$, the right-hand side for 2D with $\alpha=3.6$. The error bar in each graph indicates the effect on η when an error of 5% enters in the determination of ξ_M; this would be a systematic error, shifting all points simultaneously.

values in 1D and 2D. The graphs clearly illustrate the scaling and nonscaling regions; in particular, the straight lines in these plots correspond to uncorrelated Miller-Abrahams hopping, so the currents in the scaling region are well below that level. The interpretation is that easy Miller-Abrahams hops will be passed recurrently (and hence put in series) before a charge carrier escapes from a local region, and more frequently so the easier the hop. By contrast, difficult Miller-Abrahams hops will not likely be revisited. The distinction between "easy" and "difficult" effective bonds follows self-consistently from the temperature-dependent average mobility μ^*, and leads to the crossover from a renormalized and scaling distribution $\mu_<$ to an exponential tail $\mu_>$, separated by the Mott scale.

V. CROSSOVER AND CONVERGENCE AT LOW TEMPERATURES

The expressions $\mu_<$ and $\mu_>$ are only asymptotically equal to $\mu(R,\varepsilon)$ sufficiently below and above $\alpha R_M+\beta\varepsilon_M$, respectively. The sharpness of the crossover to negligible contributions beyond ξ_M can be characterized, e.g., by the value of the residue

$$\eta=\frac{1}{\mu^*(\beta)}\int_{\alpha R+\beta|\varepsilon|>2\xi_M} d\mathbf{R}d\varepsilon\mu_<(R,\varepsilon;\beta), \tag{14}$$

which still has to be proven small. The integration in Eq. (14) straightforwardly gives a prefactor $(\alpha^d\beta/\varrho_F)^{-1}$, which vanishes linear in T. However, the integrand includes a factor $(\alpha R)^2$ and the integration also runs over the areas $\alpha R+\beta|\varepsilon|>2\xi_M$ with $\alpha R<\xi_M$ or $\beta|\varepsilon|<\xi_M$, which leads to a power series in ξ_M in the numerator of the prefactor. Still, since asymptotically $\xi_M^{d+1}\sim l^{d+1}\sim\beta$ we conclude that η is indeed small, but only vanishes linear in ξ_M^{-1} when $T\to 0$ or $\alpha^{-1}\to 0$:

$$\eta=\frac{h(1,1)}{(\alpha^d\beta/\varrho_F)}(c_{-2}\xi_M^{-2}+c_{-1}\xi_M^{-1}+\cdots c_d\xi_M^d)\approx\frac{h(1,1)}{H}\frac{c_d}{\xi_M}. \tag{15}$$

For increasing T or α^{-1} the contribution from the outer integration region increases, and hence the deviation from scaling near (R_M,ε_M) will increase, as was observed in Fig. 3; note that in constructing Figs. 3 and 5 the limit form of Eq. (12) has already been used, which introduces additional errors of $O(\eta)$.

Obviously the crossover and the numerical corrections to scaling for increasing temperature and delocalization are beyond the present asymptotic theory and deserve further study. We have nevertheless checked the values of η vs temperature in 1D and 2D in Fig. 6 and conclude that the simulation data are consistent with Eq. (15): for larger values of β^{-1} the residue η decays to approximately zero like the leading factor at the right hand of Eq. (15), while the correction factors in Eq. (15) would bend the curves down even further in the limit $\beta^{-1}\to 0$. The latter effect will be stronger, and hence the initial convergence weaker, for higher dimensions.

VI. COMPARISON WITH RANDOM-RESISTOR AND PERCOLATION DESCRIPTIONS

For comparison with the numerical results in Ref. 18, it is important to note that our energy variable $|\varepsilon|=|\varepsilon_j-\varepsilon_i|$ differs from that considered in the random-resistor-network description,[15–17] and also used in Ref. 18 for analyzing data from the master-equation simulation. The latter energy variable will henceforth be denoted ω and reads in our notation $\omega_{ij}\equiv(|\varepsilon_i|+|\varepsilon_j|+|\varepsilon_i-\varepsilon_j|)/2$; it only corresponds exactly with Eq. (4) for energy states asymptotically far from ε_F. Still, for the dominant *critical* hops between such states—those crossing ε_F—the variables $|\varepsilon|$ and ω are identical; these hops will also be the ones to which the ansatz $\mu_>$ Eq. (7) should particularly apply. In terms of the initial and final energies ε_i, ε_j the full difference between $|\varepsilon|$ and ω is visualized in Fig. 7. It shows that where the double sum in Eq. (3) has in Eq. (6) been replaced by an integral $\int d\mathbf{R}d\varepsilon$, this would in the random-resistor variables be replaced by $\int d\mathbf{R}d\omega\omega$. The extra factor ω simply shifts the position of the peak in the hop distribution away from the horizontal axis, as was observed in Ref. 18. Also, it is clear from this extra factor ω that linear contours as considered in the regime of critical hops in Fig. 4 will not remain linear in the random-resistor variables; note that in Ref. 18 the boundary of critical hops was assumed linear in the latter variables. For further comparison with the analysis of Ref. 18 it should also be realized from Fig. 7 that the use of the energy variable $|\varepsilon|\equiv|\varepsilon_j-\varepsilon_i|$ in the energy integration, rather than $\omega_{ij}\equiv(|\varepsilon_i|+|\varepsilon_j|+|\varepsilon_i-\varepsilon_j|)/2$ (as done in Ref. 18), guarantees at equal $|\varepsilon|$, ω a faster convergence in the double summation (3) over all site energies ε_i, ε_j. These observations may explain why in Ref. 18 the 3D current distribution for low temperatures appeared to remain sub-

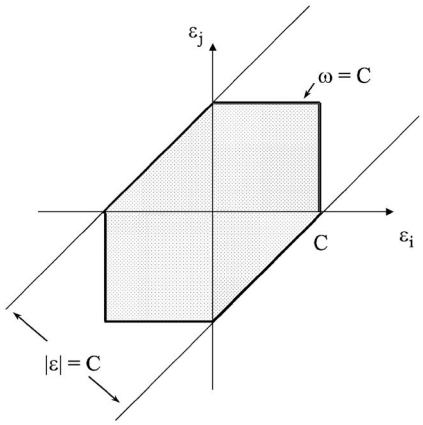

FIG. 7. Visualization of the relation between the site energies ε_i, ε_j, their energy difference ε, and the random-resistor energy variable ω. For fixed and equal upper boundaries $|\varepsilon|=\omega=C$ the integration over $|\varepsilon|$ covers a larger part of parameter space (the band between parallel lines) than that over ω (the shaded area), leading to faster convergence in the calculation of the simulated mobility.

stantial beyond the assumed linear boundary of critical-percolation hops.

Percolation arguments have extensively been used to derive and examine Mott variable-range hopping theory (see, e.g., Refs. 15–17). To make a connection, we define and compare two partial mobilities: $\mu_s^*(\xi)$ is obtained from the master equation by integrating the exact solution on the full lattice only partly, up to the variable ξ (as in the scaling approach); by contrast, $\mu_p^*(\xi)$ is the mobility obtained by exactly solving the master equation for the corresponding partial lattice, i.e., with lattice bonds beyond ξ removed (as in the percolation approach). In Fig. 8 $\mu_s^*(\xi)$ reaches at the point $\xi=\xi_M$ about 90% of its saturation value, and we have verified in Fig. 6 that for lower T it gets near 100%, consistent with the scaling theory. This point is very close to the threshold ξ_c where $\mu_p^*(\xi)$ starts to show percolation; below the latter point $\mu_p^*(\xi)$ vanishes. So whereas the characteristic scales ξ_M, ξ_c [and hence the corresponding T-dependent ex-

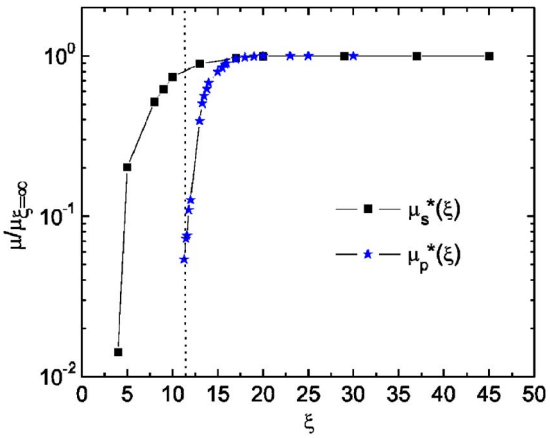

FIG. 8. (Color online) Comparison between the mobilities $\mu_s^*(\xi)$ and $\mu_p^*(\xi)$ as a function of ξ (values of 2ξ are indicated), where $\mu_s^*(\xi)$ and μ_p^* are defined in the text, for a 2D system with $\alpha=3.6$ and $(\beta\alpha^2/\varrho_F)^{1/3}=9.3$. The dotted line indicates the position of ξ_M.

ponentials $\exp(-2\xi)$] seem close, the percolation picture cannot account for the level of conductivity, since removing bonds rather than ignoring their effective current contribution in the numerical integration renders a different network with an essentially different current distribution.

It should be emphasized that the original percolation approach of Refs. 15–17 applies to a random-resistor network in the variables R, ω, whereas in Eq. (3) we consider data from the master equation, and use the variables R, ε. An additional difference between the two models is that in calculating the overall conductance from Eq. (5), the random-resistor calculation ignores the obviously present correlation between the hop distance $|\mathbf{R}_{ij}|$ and hop rate $G_{ij}V_{ij}$. Furthermore, the treatment of Ref. 17 derives the prefactor of Mott's law explicitly from the properties of the just-percolating network, with many network bonds removed; as demonstrated in Fig. 8 such removal of bonds may have an effect, with consequences different for slightly different models. So we conclude that quantitative numerical differences will remain between our master-equation results and the outcome of the percolation approach. An extensive numerical study of the percolation behavior on a random-resistor network has been performed recently.[26]

VII. THE ROLE OF FLUCTUATIONS

A striking conclusion from Fig. 8 is that while the integral of the current distribution up to the Mott scale ξ_M approaches the total current, with increasing accuracy for lower temperatures, bonds just beyond this scale may not simply be cut. An insight into this may already be obtained from Fig. 5, which shows that even at such temperatures there exists a regime beyond ξ_M in which the current distribution still deviates somewhat from an exponential, i.e., hops are still correlated. The explanation is that the very occurrence of variable-range hopping points at a local lack of accessible energy levels, i.e., to poor spatial statistics. Detailed balance in the master equation can only give Fermi statistics at the expense of correlated local chemical potentials and currents; these are the correlated potentials and currents observed in the simulations.[18] A first estimate for a length scale R_{fl} beyond which homogeneous Fermi statistics occurs and correlations will vanish is

$$\varrho_F[R_{fl}(\beta)]^d \gg \beta. \tag{16}$$

Comparison with the Mott condition shows that a scale thus defined will indeed be much larger than the Mott scale. In terms of the dimensionless variable ξ we have for the ratio of scales

$$\xi_{fl}/\xi_M \gg \xi_M^{1/d} \sim \beta^{1/[d(d+1)]}, \tag{17}$$

which weakly diverges in the limit of low temperatures. [Note that the existence of a regime beyond ξ_M with deviation from exponential behavior actually necessitates a refinement of the asymptotic analysis leading from Eq. (14) to Eq. (15), i.e., to a proof that the residue η vanishes. However, it may be easily verified that in a corrected expression (14) the integrand remains dominated, and may be bounded from above, by an exponential, leading to the same arguments.]

So we propose a picture that beyond a scale ξ_{fl} much larger than the Mott scale single uncorrelated hops will always be possible within a distance k_BT from the sample-averaged Fermi level, and that on such a scale the system obeys homogeneous Fermi statistics. Below ξ_{fl} some very large hops $(R_{ij},\varepsilon_{ij})$ may occasionally become important to avoid unfavorable local energy regions, but this reflects local fluctuations in the network properties and in the resulting VRH currents. In this regime all bonds (i,j) of one type $(R_{ij}=R,\ |\varepsilon_{ij}|=|\varepsilon|)$ together may contribute little to the total current at low temperature, but cutting them all—as in the percolation approach—implies cutting also the locally important ones. Inevitably this will be at the expense of some reduction in the total current; however, in the low-temperature limit this effect remains dominated by the exponential tail in the current distribution, and vanishes faster than the total current itself. Only below the Mott scale ξ_M, which self-consistently separates a scaling-dominated regime from an exponential-dominated regime, all bonds become essential in recovering the total low-temperature current of the full network; here the VRH mechanism, with hops maximally of length R_M, is necessary to overcome the large average spacing between local energy levels, in order to percolate across regions of size R_{fl}.

It is interesting to note that the spatial fluctuations discussed here will become practically relevant in real samples of reduced dimensions L with $R_M \ll L \lesssim R_{fl}$, since the finite sample size then affects the equilibration condition (16) and hence cuts off part of the potentially contributing energy states and VRH paths; effectively, this forces the charge through steeper, wider-spaced energy landscapes with significant sample-to-sample variations. On the basis of Eq. (16) one may guess that in a sample of size L^d the hop-energy scale $(\sim \varrho_F^{-1/d+1})$, and hence the fluctuations in the Mott energy and Mott length (and thus also the fluctuations in the exponent of the mobility) become proportional to $L^{-d/d+1}$; assuming that for $R_M \ll L \ll R_{fl}$ exponential localization is valid, i.e., that the conductance scales exponentially with linear system size L, we guess that the logarithm of the conductance would then fluctuate proportional to $L^{1/d+1}$. In fact, the fluctuations discussed in this paper are essentially the same as the geometrical "intrinsic fluctuations in the Mott hopping process" originally discussed by Lee[23] and Serota, Kalia, and Lee[24] in the context of VRH conduction through finite 1D samples, and later extended to 2D configurations[27] and to quantum effects.[28] The case $d=1$ thereby creates special logarithmic size-dependent features, leading to strong mesoscopic-conductance variations as observed, e.g., in narrow-channel MOSFET devices.[29]

VIII. CONCLUSIONS

To summarize, in (R,ε) space the region of relevant Mott hops bounded by $\xi_M(\beta)$ is a scaling regime, with a self-organized hop distribution only determined by scaled variables. In this regime of relatively easy passages the *effective hop* probabilities are well below the corresponding *single-hop* Miller-Abrahams factors; this can be understood as being due to iterative hops before local escape. At the boundary there is a crossover, via a regime with current fluctuations intrinsic to VRH, towards a Miller-Abrahams-type single-bond hopping distribution, i.e., to an exponential cutoff. The scaling regime diverges for $T \to 0$. Most-frequent hops occur around the origin while there is a peak of dominant contributions well inside the scaling boundary. The position of the boundary, determined by a Mott-type condition for a critical hop, is temperature-sensitive, and due to scaling this temperature dependence enters μ^* in a form as envisaged by Mott.

ACKNOWLEDGMENTS

The authors acknowledge the support of H. B. Brom and H. P. Huinink throughout this work, and the important contributions of P. A. Bobbert to the simulation results. One of the authors (M.A.J.M.) acknowledges a stimulating discussion with B. I. Shklovskii. This work forms part of the research program of the Dutch Polymer Institute (project 274).

*Present address: Philips Research Eindhoven.
†Author to whom correspondence should be addressed. Electronic mail: m.a.j.michels@tue.nl

[1] For a review see, e.g., T. G. Castner, in *Hopping Transport in Solids*, edited by M. Pollak and B. I. Shklovskii (North-Holland, Amsterdam, 1991), p. 1.
[2] A. Faggionato, H. Schulz-Baldes, and D. Spehner, Commun. Math. Phys. **263**, 21 (2006).
[3] T. Vuletic, B. Korin-Hamzic, S. Tomic, B. Gorshunov, P. Haas, M. Dressel, J. Akimitsu, T. Sasaki, and T. Nagata, Phys. Rev. B **67**, 184521 (2003).
[4] H. C. F. Martens, I. N. Hulea, I. Romijn, H. B. Brom, W. F. Pasveer, and M. A. J. Michels, Phys. Rev. B **67**, 121203(R) (2003).
[5] D. N. Tsigankov and A. L. Efros, Phys. Rev. Lett. **88**, 176602 (2002).
[6] V. I. Arkhipov, E. V. Emelianova, and G. J. Adriaenssens, Phys. Rev. B **65**, 165110 (2002).
[7] Z. G. Yu and X. Song, Phys. Rev. Lett. **86**, 6018 (2001).
[8] T. G. Castner, Phys. Rev. B **61**, 16596 (2000).
[9] J. A. Reedijk, H. C. F. Martens, H. B. Brom, and M. A. J. Michels, Phys. Rev. Lett. **83**, 3904 (1999).
[10] M. C. J. M. Vissenberg and M. Matters, Phys. Rev. B **57**, 12964 (1998).
[11] N. V. Lien and R. Rosenbaum, Phys. Rev. B **56**, 14960 (1997).
[12] N. F. Mott, J. Non-Cryst. Solids **1**, 1 (1968); Philos. Mag. **19**, 835 (1969).
[13] A. Miller and E. Abrahams, Phys. Rev. **120**, 745 (1960).
[14] A. L. Efros and B. I. Shklovskii, J. Phys. C **8**, L49 (1975).
[15] V. Ambegaokar, B. I. Halperin, and J. S. Langer, Phys. Rev. B **4**,

2612 (1971).
[16] M. Pollak, J. Non-Cryst. Solids **11**, 1 (1972).
[17] B. I. Shklovskii and A. L. Efros, *Electronic Properties of Doped Semiconductors* (Springer, Berlin, 1985).
[18] W. F. Pasveer, P. A. Bobbert, H. P. Huinink, and M. A. J. Michels, Phys. Rev. B **72**, 174204 (2005).
[19] Z. G. Yu, D. L. Smith, A. Saxena, R. L. Martin, and A. R. Bishop, Phys. Rev. B **63**, 085202 (2001).
[20] P. N. Butcher, in *Linear and Nonlinear Electronic Transport in Solids*, edited by J. T. Devreese and V. E. van Doren (Plenum, New York, 1976), p. 348.
[21] J. A. McInnes and P. N. Butcher, Philos. Mag. B **39**, 1 (1979).
[22] I. I. Fishchuk, A. Kadashchuk, and H. Baessler, Phys. Status Solidi C **3**, 271 (2006).
[23] P. A. Lee, Phys. Rev. Lett. **53**, 2042 (1984).
[24] R. A. Serota, R. K. Kalia, and P. A. Lee, Phys. Rev. B **33**, 8441 (1986).
[25] B. Movaghar and W. Schirmacher, J. Phys. C **14**, 859 (1981).
[26] H. P. Huinink, P. A. Bobbert, W. F. Pasveer, and M. A. J. Michels, Phys. Rev. B **73**, 224204 (2006).
[27] R. A. Serota, Solid State Commun. **67**, 1031 (1988).
[28] A. M. Somoza, M. Ortuno, and J. Prior, Europhys. Lett. **70**, 649 (2005).
[29] A. B. Fowler, A. Hartstein, and R. A. Webb, Phys. Rev. Lett. **48**, 196 (1982).